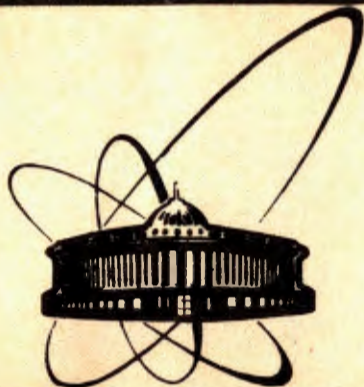


92-249



СООБЩЕНИЯ
ОБЪЕДИНЕННОГО
ИНСТИТУТА
ЯДЕРНЫХ
ИССЛЕДОВАНИЙ
ДУБНА

E1-92-249

V.I.Yurevich, R.M.Yakovlev*, V.G.Lyapin*,
I.O.Tsvetkov*, A.V.Daniel*

EXPERIMENTAL SETUP FOR STUDY OF HADRON
AND HARD PHOTON PRODUCTION
IN NUCLEUS-NUCLEUS COLLISIONS

*V.G.Khlopov Radium Institute, Sankt-Petersburg, Russia

1992

Introduction

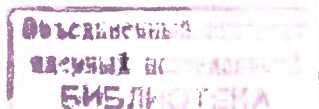
Nucleus-nucleus collisions at intermediate and high energies are a very interesting and quickly developing branch of modern nuclear physics connected with the research of new extreme states of nuclear matter. These high-dense and high-temperature nuclear matter states produced in central collisions have a very short lifetime and disintegrate with hard photon and hadron emission [1].

The described experimental setup has been constructed to study the possibility and conditions of strengthening the display of the effect of new nuclear matter form and its the investigation. The measurements of hadron and hard photon spectra give important information about all stages of the evolution process of a produced nuclear system. So in the future we plan to study $\gamma/\pi/n/p/d/t$ production differential cross sections in a broad region of energy, colliding nucleus mass and emission angles.

Our setup placed on external heavy-ion beam channel N38 of the JINR Synchrophasotron consists of a tandem of the $\Delta E-E$ and $t-E$ spectrometers. The main characteristics of this setup and the used experimental technique are described in this paper.

Experimental area

A general view of the setup and a schematic drawing of target-detector arrangement of the spectrometers are shown in figs.1 and 2, respectively.



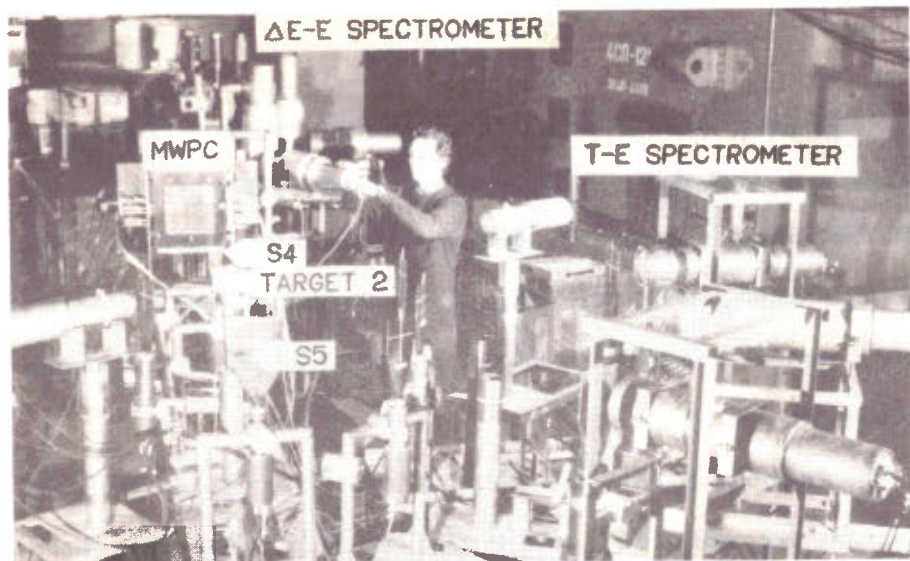


Fig.1 General view of the experimental setup.

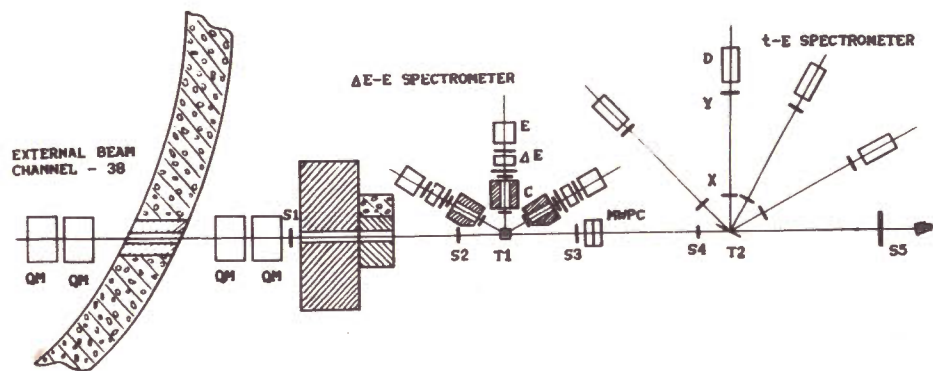


Fig.2 Schematic drawing of target-detector arrangement of the ΔE -E and t-E spectrometers.

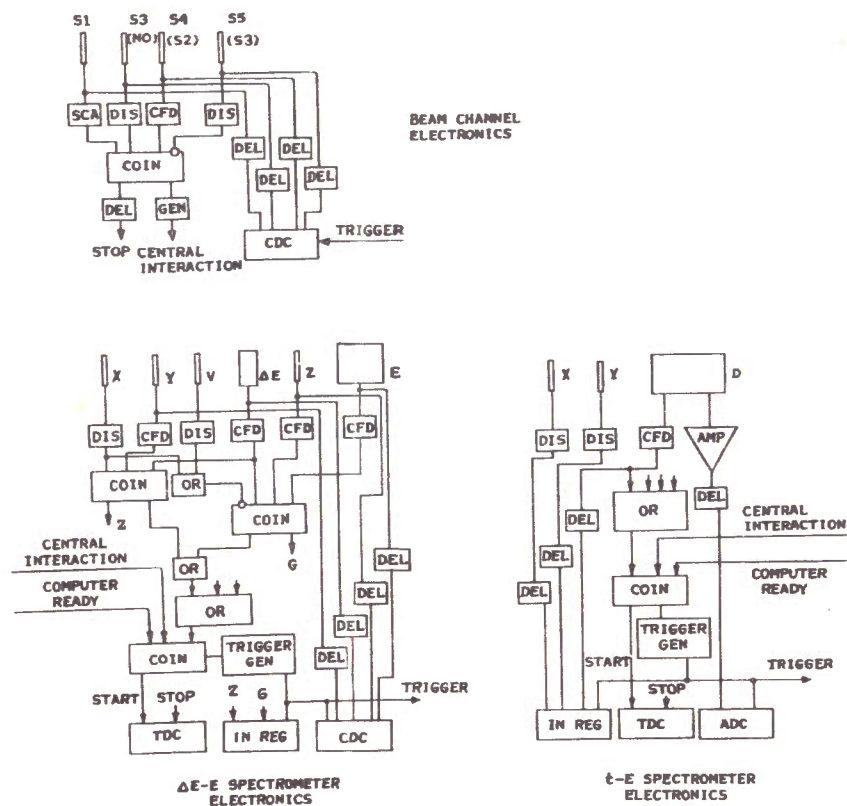


Fig.3 Scheme of the spectrometer electronics:

DIS - fast discriminator, CFD - constant fraction discriminator,

DEL - delay, COIN - coincidence scheme, GEN - generator,

AMP - amplifier, CDC - charge-to-digital converter,

TDC - time-to-digital converter, ADC - analog-to-digital converter

The t-E spectrometer is placed after the ΔE -E spectrometer along the beam direction. The first ΔE -E spectrometer has been designed for the investigation of hard photon emission with three identical gamma-telescopes based on large volume NaJ(Tl) detectors. Charged hadrons can be also measured by the ΔE -E technique. The second spectrometer is a time-of-flight spectrometer of neutrons and charged hadrons with charged particle separation by the t-E method. Four identical detector systems with plastic scintillators are located at different angles. Each spectrometer has its target, and both can operate independently. A large experimental hall and the absence of essential scattering masses around the setup allow one to get good background conditions.

The spectrometer electronics is in an experimental room spaced at about 30 m from the experimental area. A simplified circuit diagram of the electronics used for data recording is schematically shown in fig.3. All CAMAC electronics manufactured by the JINR is connected to a computer, and experimental information is stored event by event on magnetic tape for subsequent off-line data analysis.

Heavy-ion beam

In the experimental area the heavy-ion beam passing through two quadrupole magnets (QM) is focused between targets T_1 and T_2 . The beam spot is typically $10 \div 15$ mm (FWHM) in the vertical and horizontal directions. The position and the profile of the beam were monitored by

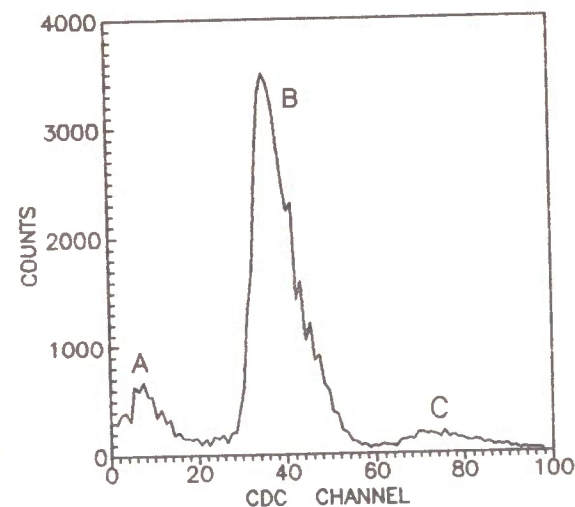


Fig.4 Pulse height distribution for beam counter S4 measured with a ^{12}C -ion beam.

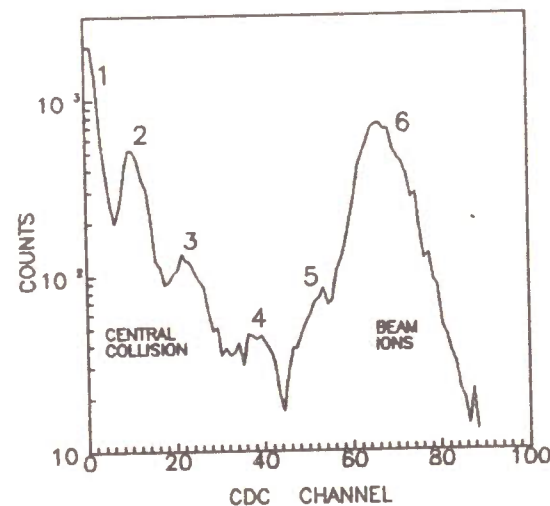


Fig.5 Pulse height distribution for beam counter S5 measured with a ^{12}C -ion and a thin lead target. Figures correspond to the charge of projectile fragments.

means of a multiwire proportional chamber (MWPC). The beam intensity is typically of the order of a few 10^5 ions per pulse. The accelerator runs in a special operation mode providing 20 ns micropulses following one after another in about 300 ns with an even distribution within a wide time interval of about 400 ms. The Synchrotron repetition rate is 1 pulse in about 8 s.

Beam intense monitoring and beam analysis are carried out by a system of beam counters (S1÷ S5) with 3 ÷ 5-mm plastic scintillators. A Signal "beam" is given by the following coincidences of beam counter pulses:

$$\text{"Beam"} = \begin{cases} S1 * S2 - \text{for } \Delta E\text{-}E \text{ spectrometer;} \\ S1 * S2 * S4 - \text{for t-E spectrometer} \end{cases}$$

A special high-voltage circuit is used to provide the required stability at high counting rates. For a beam intensity of more than 10^5 ions per accelerator pulse the possibility of the presence of more than one ion within a micropulse must be taken into account. Moreover, the inelastic nuclear interactions of incident ions in the counter scintillators should be also take into account for a background decrease. So, the beam analysis is performed to measure the pulse height distribution from the beam counters by charge-to-digital converters (CDC). The pulse height distribution for beam counter S4 measured with a ^{12}C -ion beam is shown in fig.4: the peak (B) corresponds to single particle micropulses, the broad peak (C) is micropulses with two or more ions and events with low pulse heights, (A)

corresponds to the background of secondary charged particles produced in the scintillators, air and also in target T_1 by beam ions. The separation of events corresponding to single ion micropulses allows one to increase beam intensity and to decrease background essentially.

Beam counters S3 (for the $\Delta E\text{-}E$ spectrometer) and S5 (for the t-E spectrometer) are used to obtain information about the inelasticity of nucleus-nucleus interactions. The typical pulse height distribution of ^{12}C projectile fragments measured with a thin lead target is given in fig.5.

A few peaks corresponding to nuclear fragments with different charge can be seen in this figure, where the main broad peak is carbon ion events ($Z=6$).

The selection of low pulse height events (projectile low-charged fragments) corresponds to the central collision region. The projectile fragments are detected by counters S3 (S5) in the forward direction at angles smaller than 5 deg.

$\Delta E\text{-}E$ Spectrometer

The detector system of each scintillation telescope of the $\Delta E\text{-}E$ spectrometer is given in table 1.

Table 1. Detector system of the scintillation telescope of the ΔE -E spectrometer.

Detector	Scintillator	Signal
X	100 * 100 * 3mm plastic	timing
Y	80 * 80 * 5mm plastic	timing,pulse height
V	150 * 150 * 5mm plastic	timing(veto-counter)
ΔE	140 * 140 * 40mm NaJ(Tl)	timing,pulse height
Z	130 * 130 * 5mm plastic	timing
E	$\phi 150 * 150$ mm NaJ(Tl)	timing,pulse height

The first NaJ(Tl) detector (ΔE) 1.56 X_0 in thickness and is a high-energy gamma-ray active converter. The electron-photon cascade passing through the thin plastic counter (Z) is absorbed in the large NaJ(Tl) detector (E).

So, the gamma-event is a $\bar{V} * \Delta E * Z * E$ coincidence producing a signal "G". The charged particle signal "Z" is given by coincidence of pulses of three detectors (X,Y and ΔE). The ΔE detector is located at a 50-cm distance from target T1. The lead collimator (the thickness is 20 cm and the aperture $\phi 6$ cm) is between the X and Y counters, and photons fall only on the central part of the front surface of the detector-converter (ΔE). This gamma-telescope overlapping the energy region from 30 to 300 MeV has been calibrated using cosmic muons. The study of hard photon detection by the gamma-telescope has been performed by the GEANT3 code [2]. The calculated pulse height response functions of the ΔE and E detectors and the summary response for 180-MeV incident photons are given in fig.6. The telescope response to 90-, 180- and 300-MeV photons is given in fig.7. The energy dependence of the gamma-telescope efficiency is presented in fig.8.

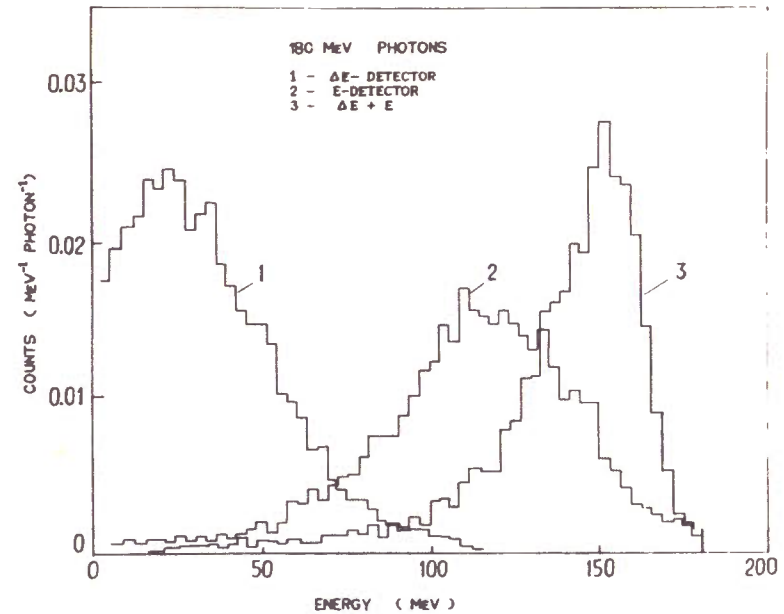


Fig.6 Response distributions of the ΔE (1) and E (2) detectors based on large NaJ(Tl) crystals and a ($\Delta E+E$) response of the gamma-telescope (3) for 180-MeV photons.

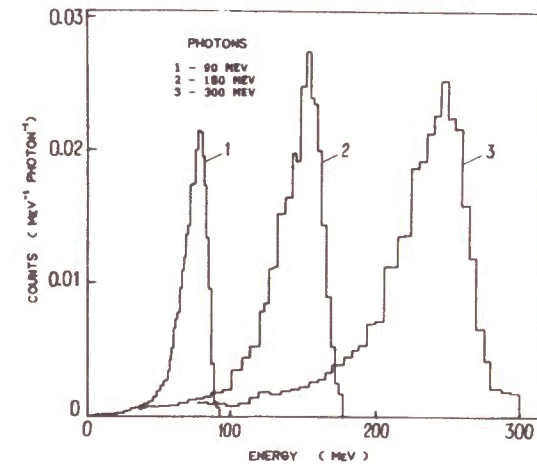


Fig.7 Response distributions of gamma-telescope for 90-, 180- and 300-MeV photons.

Table 2. A comparison of the hard photon spectrometers.

Year [reference.]	γ -detector	E_γ (MeV)	ϵ_γ (%)	FWHM (%)	FWHM(TOP) (ns)
	present detector system	30-300	15-43	20	0.7
1987 [3]	veto-counter BaF ₂ ($\phi 10 \times 14$ cm)	8-85		15-30	0.7
1988 [4]	veto-counter, BaF ₂ (6 * 4 * 1cm), two NE102(2mm), NaJ(Tl)($\phi 15 \times 20$ cm)	> 20			
1988 [5]	veto-counter, the set from five Pb-glass detectors	20-150	9-20	25-35	2.5
1988 [6]	veto-counter, BaF ₂ (60cm ³) BGO(750cm ³)			14	0.5
1989 [7]	veto-counter, Ca/SCG1-C glass (0.5 X ₀ converter), two MWPC,plastic, SCG1-C glass (15 * 15 * 42.5cm)	20-300	20		

Table 3. Telescope detector system of the t-E spectrometer.

Detector	Scintillator	Signal
X	100 * 100 * 3mm plastic	timing
Y	130 * 130 * 5mm plastic	timing
D	$\phi 120 \times 200$ mm plastic	timing,pulse-height

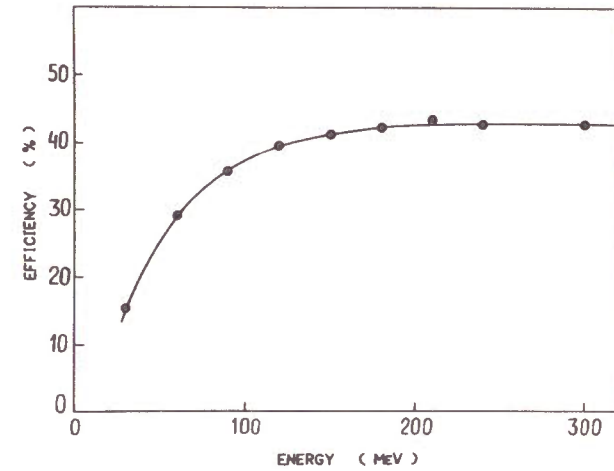


Fig.8 Energy dependence of gamma-telescope efficiency.

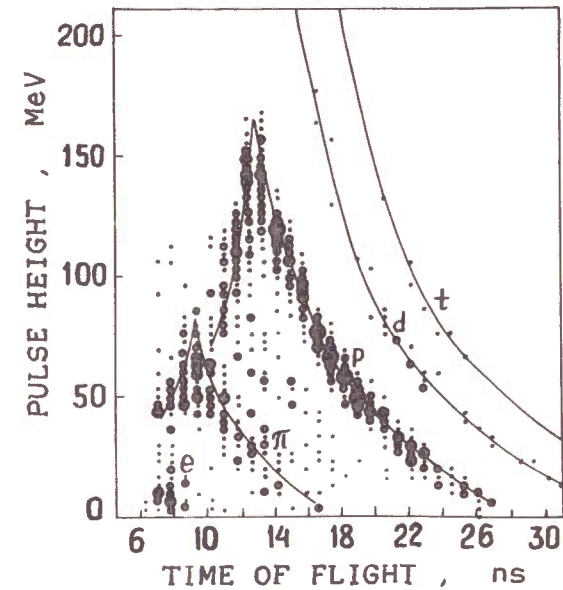


Fig.9 The t-E plot measured at 30° with 1-GeV*A ⁶Li-ions and a carbon target: points - experiment, curves - calculation.

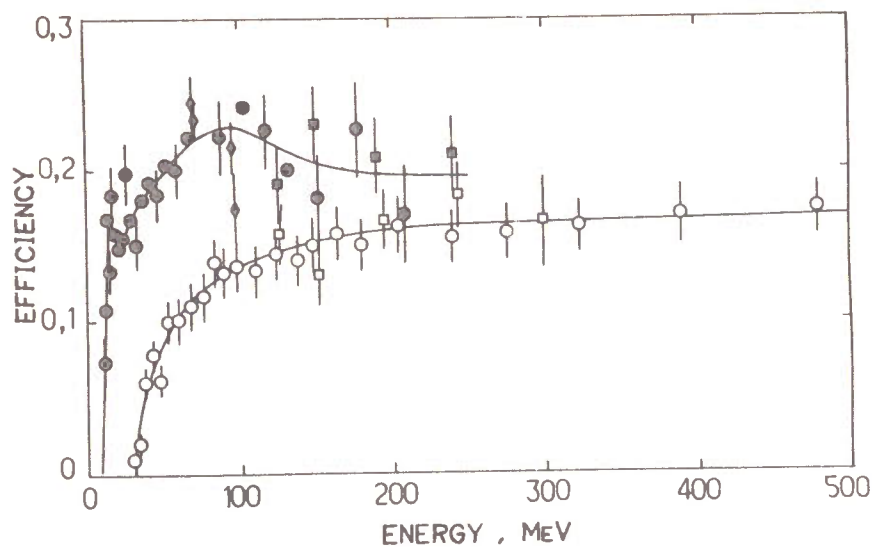


Fig.10 Efficiency of neutron detector for two threshold values 10 and 30 MeV.

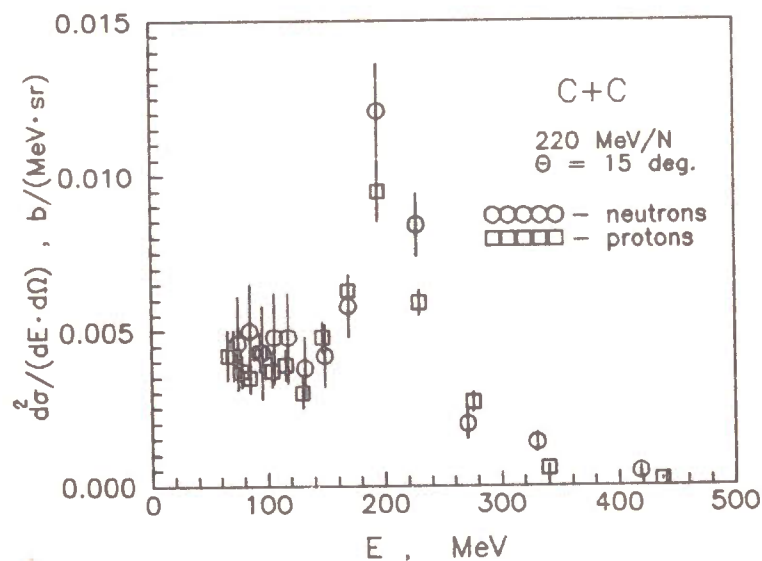


Fig.11 Double differential cross section of neutron and proton production in $C + C$ collisions at $\theta_{ab} = 15^\circ$ for beam energy 220 MeV/N.

A strong background discrimination is performed by (1) a fast coincidence of pulses from the ΔE , Z and E detectors within 20 ns; (2) the use of short time interval of about 1 ns on the time-of-flight scale and (3) veto-counter charged particle discrimination. The use of a thin Cherenkov counter instead of a Z plastic counter can give a stronger discrimination of high-energy neutron background. In table 2 our gamma-telescope is compared with other setups.

t-E spectrometer

The t-E spectrometer is used for time-of-flight measurements of double differential cross sections of hadron production with the off-line separation of π^\pm , p, d and t by t-E (time of flight - pulse height) analysis. The spectrometer is the same as the setup described in ref.[8]. Charged particles are measured by the scintillation telescope which consists of two counters (X,Y) and an E detector (D). The counters Y are used as veto-counters in off-line neutron data processing. The characteristic of the telescope detector system is given in table 3. The t-E plot for the interaction of 1-GeV*A ${}^6\text{Li}$ -ions with a carbon target is shown in fig.9. This figure demonstrates a good separation of single-charged particles by the off-line t-E method. The efficiency of the neutron detector for two threshold values of 10 and 30 MeV is shown in fig.10.

An example of the measurement results obtained in $C + C$ collisions at angle $\theta_{lab} = 15^\circ$ for a beam energy of 220 MeV/N is shown in fig.11. Both proton and neutron energy spectra have a peak at energy which is about beam energy per nucleon and a high-energy tail up to double projectile nucleon energy.

References

- [1] Nagamiya S. - University of Tokyo Report UTPN-209; 210, 1984.
- [2] Brun R. et al. - GENT 3 Data Handling Division, CERN DD/EE/84-1, 1987.
- [3] Hingmann et al. - Phys. Rev. Lett. v.58 (1987) 759.
- [4] Kwato Njock M. et al. - Phys. Lett. B v.207 (1988) 269.
- [5] Tam C.L. et al. - Phys. Rev. C v.38 (1988) 2526.
- [6] Arctaedins Th. et al. - 3 ed Inter. Conf. on Nucleus-Nucleus Collisions, 1988 Saint-Malo, France (1988) 94.
- [7] Chiavassa E. et al. - Nuovo Cimento A v.101 (1989) 805.
- [8] Bayukov Yu.D. et al. - Preprint ITEP-159; ITEP-16, M., 1980.

Received by Publishing Department
on June 15, 1992.

WILL YOU FILL BLANK SPACES IN YOUR LIBRARY?

You can receive by post the books listed below. Prices — in US \$, including the packing and registered postage.

D13-85-793	Proceedings of the XII International Symposium on Nuclear Electronics, Dubna, 1985.	14.00
D1,2-86-668	Proceedings of the VIII International Seminar on High Energy Physics Problems, Dubna, 1986 (2 volumes)	23.00
D3,4,17-86-747	Proceedings of the V International School on Neutron Physics. Alushta, 1986.	25.00
D9-87-105	Proceedings of the X All-Union Conference on Charged Particle Accelerators. Dubna, 1986 (2 volumes)	25.00
D7-87-68	Proceedings of the International School-Seminar on Heavy Ion Physics. Dubna, 1986.	25.00
D2-87-123	Proceedings of the Conference "Renormalization Group-86". Dubna, 1986.	12.00
D2-87-798	Proceedings of the VIII International Conference on the Problems of Quantum Field Theory. Alushta, 1987.	10.00
D14-87-799	Proceedings of the International Symposium on Muon and Pion Interactions with Matter. Dubna, 1987.	13.00
D17-88-95	Proceedings of the IV International Symposium on Selected Topics in Statistical Mechanics. Dubna, 1987.	14.00
E1,2-88-426	Proceedings of the 1987 JINR-CERN School of Physics. Varna, Bulgaria, 1987.	14.00
D14-88-833	Proceedings of the International Workshop on Modern Trends in Activation Analysis in JINR. Dubna, 1988	8.00
D13-88-938	Proceedings of the XIII International Symposium on Nuclear Electronics. Varna, 1988	13.00
D17-88-681	Proceedings of the International Meeting "Mechanisms of High- T_c Superconductivity". Dubna, 1988.	10.00
D9-89-52	Proceedings of the XI All-Union Conference on Charged Particle Accelerators. Dubna, 1988 (2 volumes)	30.00
E2-89-525	Proceedings of the Seminar "Physics of e^+e^- Interactions". Dubna, 1988.	10.00
D9-89-801	Proceedings of the International School-Seminar on Heavy Ion Physics. Dubna, 1989.	19.00
D19-90-457	Proceedings of the Workshop on DNA Repair on Mutagenesis Induced by Radiation. Dubna, 1990.	15.00